

E. Arik<sup>a</sup>, O. Çakır<sup>b</sup>, S. A. Çetin<sup>a</sup> and S. Sultansoy<sup>c,d</sup>

<sup>a</sup> *Bogazici University, Faculty of Sciences, Department of Physics,  
80815, Bebek, Istanbul, Turkey*

<sup>b</sup> *Ankara University, Faculty of Sciences, Department of Physics,  
06100 Tandogan, Ankara, Turkey*

<sup>c</sup> *Gazi University, Faculty of Arts and Sciences, Department of Physics,  
06500, Teknikokullar, Ankara, Turkey*

<sup>d</sup> *Azerbaijan Academy of Sciences, Institute of Physics,  
H. Cavid av., 33, Baku, Azerbaijan*

Resonant production of the first generation vector diquarks at the CERN Large Hadron Collider (LHC) have been investigated. It is shown that the LHC will be able to discover vector diquarks with masses up to 9 (8) TeV if coupling  $\alpha_D \simeq \alpha_s(\alpha_{em})$ .

## I. INTRODUCTION

The existence of at least three fermion families naturally leads to the hypothesis that they are made up of more fundamental constituents frequently called preons [1]. Today, the compositeness should be considered as a candidate for beyond the standard model (BSM) physics on the same footing as SUSY. Moreover, some assumptions made in order to get rid of huge number of free parameters in three family MSSM have natural explanation (see [2] and references therein) in the framework of preonic models. These models predict a rich spectrum of new particles with unusual quantum numbers at high energies such as excited quarks and leptons, diquarks, dileptons, leptoquarks, leptogluons, sextet quarks, octet bosons etc. In preonic models, diquarks are as natural as leptoquarks [3]. They are colored objects having integer-spin and baryon number  $|B| = 2/3$ . Diquarks are also predicted in the framework of superstring-inspired  $E_6$  models [4].

Recent collider limits on the diquark masses come from Tevatron data which exclude the region  $290 < M < 420$  GeV (for  $E_6$  diquarks) [5]. Diquark production at  $e^+e^-$  colliders,  $ep$  colliders and  $p\bar{p}$  colliders have been analyzed in [6], [7] and [8], respectively. Recently, the resonance production of scalar diquarks at CERN LHC has been studied in [9].

In this work, the sensitivity of LHC to composite vector diquark production is estimated. In section II, interaction lagrangian and quantum numbers of diquarks are discussed. Decay width and production cross section of a vector diquark at the CERN LHC are considered in section III. Then, in section IV, vector diquark signal and corresponding backgrounds are analyzed. Finally, in section V we give some conclusions and remarks.

## II. INTERACTION LAGRANGIAN AND CLASSIFICATION

A model independent, most general, effective  $SU(3)_C \times SU(2)_W \times U(1)_Y$  invariant lagrangian for diquarks has the form [9]:

$$\begin{aligned}
 L = & g_{1L} \bar{q}_L^c i\tau_2 q_L D_1^c + g_{1R} \bar{u}_R^c d_R D_1^c + \tilde{g}_{1R} \bar{d}_R^c d_R \tilde{D}_1^c + \tilde{g}'_{1R} \bar{u}_R^c u_R \tilde{D}'_1^c + g_{3L} \bar{q}_L^c i\tau_2 \vec{\tau} q_L \cdot \vec{D}_3^c \\
 & + g_2 D_{2\mu}^{cT} \bar{d}_R^c i\tau_2 \gamma^\mu q_L + \tilde{g}_2 \tilde{D}_{2\mu}^{cT} \bar{u}_R^c i\tau_2 \gamma^\mu q_L + h.c.
 \end{aligned}
 \tag{1}$$

where  $q_L = (u_L, d_L)$  and  $q^c = C\bar{q}^T$  ( $\bar{q}^c = -q^T C^{-1}$ ). For the sake of simplicity, color and generation indices are omitted. Scalar diquarks  $D_1, \tilde{D}_1, \tilde{D}'_1$  are  $SU(2)_W$  singlets and  $\vec{D}_3$  is  $SU(2)_W$  triplet. Vector diquarks  $D_2$  and  $\tilde{D}_2$  are  $SU(2)_W$  doublets. Diquarks may transform as anti-triplet or sextet under  $SU(3)_C$ . At this stage, we assume each SM generation has its own diquarks and couplings in order to avoid restrictions imposed by  $\Delta m_K$  etc.

Lagrangian (1) can be rewritten in the following more transparent form:

$$L = L_S + L_V \quad (2)$$

$$L_S = [g_{1L} (\bar{u}^c P_L d - \bar{d}^c P_L u) + g_{1R} \bar{u}^c P_R d] D_1 + \tilde{g}_{1R} \bar{d}^c P_R d \tilde{D}_1 + \tilde{g}'_{1R} \bar{u}^c P_R u \tilde{D}'_1 \\ + \sqrt{2} g_{3L} \bar{u}^c P_L u D_3^+ - \sqrt{2} g_{3L} \bar{d}^c P_L d D_3^- - g_{3L} (\bar{u}^c P_L d + \bar{d}^c P_L u) D_3^0 + h.c. \quad (3)$$

$$L_V = g_2 \bar{d}^c \gamma^\mu P_L d D_{2\mu}^1 - g_2 \bar{d}^c \gamma^\mu P_L u D_{2\mu}^2 + \tilde{g}_2 \bar{u}^c \gamma^\mu P_L d \tilde{D}_{2\mu}^1 - \tilde{g}_2 \bar{u}^c \gamma^\mu P_L u \tilde{D}_{2\mu}^2 + h.c. \quad (4)$$

where  $P_L = (1 - \gamma_5)/2$  and  $P_R = (1 + \gamma_5)/2$ . A general classification of the first generation, color  $\bar{\mathbf{3}}$  diquarks is shown in Table I.

### III. DECAY WIDTH AND PRODUCTION CROSS SECTION

For the present analysis, we will take into account the color  $\bar{\mathbf{3}}$  vector diquark  $D_2$  which couples to  $ud$ -pair as described by the effective lagrangian (4). The decay width  $\Gamma_D$ , derived from the same lagrangian, is

$$\Gamma_D = C_F \frac{g_2^2 M_D}{24\pi} \quad (5)$$

where  $C_F$  is the color factor for triplet representation and  $M_D$  is the mass of vector diquark. We will use the definition  $g_2^2 = 4\pi\alpha_D$  for numerical calculations:

$$\Gamma_D = C_F \frac{\alpha_D M_D}{6} \simeq 17 \text{ GeV} \left( \frac{C_F M_D}{1 \text{ TeV}} \right) \quad \text{for } \alpha_D = 0.1 \simeq \alpha_s \quad (6)$$

$$\simeq 1.3 \text{ GeV} \left( \frac{C_F M_D}{1 \text{ TeV}} \right) \quad \text{for } \alpha_D \simeq \alpha_{em} \quad . \quad (7)$$

In the narrow width approximation ( $\Gamma/M < 0.1$ ), the cross section of the s-channel diquark resonance production can be obtained as

$$\sigma(pp \rightarrow D_2 X) = \sum_{ab} \frac{C_F^2 \alpha_D \pi^2}{s} \int_{M_D^2/s}^1 \frac{dx}{x} f_a(x, \hat{s}) f_b\left(\frac{M_D^2}{sx}, \hat{s}\right) \quad (8)$$

where  $\hat{s} = x_a x_b s$ ,  $f_a$  and  $f_b$  are quark distribution functions of each proton. In Fig. 1, using the CTEQ5L quark distribution functions [10], the cross section versus diquark mass is plotted for coupling  $\alpha_D = \alpha_s$  and  $\alpha_D = \alpha_{em}$  at the LHC energy ( $\sqrt{s} = 14 \text{ TeV}$ ).

### IV. SIGNAL AND BACKGROUND

$D_2$ -type diquark resonance in s-channel will be formed via the subprocess  $u + d \rightarrow D_2 \rightarrow u + d$ . Therefore, the signal will contain two hard jets in the final state. Considering only the interference with the t-channel gluon exchange, the following differential cross section is obtained:

$$\frac{d\hat{\sigma}}{d\hat{t}}(q_i q_j \rightarrow q_i q_j) = C_F^2 \pi \left[ \frac{\alpha_D^2 (\hat{s} + \hat{t})^2}{\hat{s}^2 [(\hat{s} - M_D^2)^2 + M_D^2 \Gamma_D^2]} \right. \\ \left. + \frac{2\alpha_s^2 (2\hat{s}^2 + \hat{t}^2 + 2\hat{s}\hat{t})}{\hat{s}^2 \hat{t}^2} - \frac{2\alpha_D \alpha_s}{\hat{t}} \frac{(\hat{s} + \hat{t})^2 (\hat{s} - M_D^2)}{\hat{s}^2 [(\hat{s} - M_D^2)^2 + M_D^2 \Gamma_D^2]} \right] \quad . \quad (9)$$

At the LHC, QCD processes contributing to two jet final states and their integrated cross sections are given in Table II. The values in Table II have been generated by PYTHIA 6.1 [11] at parton level with various  $p_T$  cuts.

The cross section as a function of the dijet invariant mass  $M_{jj}$  with the rapidity cut  $|y_{1,2}| \leq Y$ , where  $y_1$  and  $y_2$  are rapidities of the massless final quarks, is given by

$$\begin{aligned}
\frac{d\sigma}{dM_{jj}} &= \frac{M_{jj}^3}{2s} \int_{-Y}^Y dy_2 \int_{y_1^{\min}}^{y_1^{\max}} dy_1 \frac{1}{\cosh^2 y^*} \\
&\times [f_{u/A}(x_u, Q^2) f_{d/B}(x_d, Q^2) \frac{d\hat{\sigma}}{d\hat{t}}(\hat{s}, \hat{t}, \hat{u}) \\
&+ f_{d/A}(x_d, Q^2) f_{u/B}(x_u, Q^2) \frac{d\hat{\sigma}}{d\hat{t}}(\hat{s}, \hat{u}, \hat{t})]
\end{aligned} \tag{10}$$

with

$$\begin{aligned}
y^* &= (y_1 - y_2)/2, & y^b &= (y_1 + y_2)/2 \\
x_u &= \sqrt{\tau} e^{y^b}, & x_d &= \sqrt{\tau} e^{-y^b} \\
\hat{s} &= x_u x_d s, & \hat{t} &= -x_u p_T \sqrt{s} e^{-y_1}, & \hat{u} &= -x_d p_T \sqrt{s} e^{y_1} \\
y_1^{\min} &= \max(-Y, \log \tau - y_2), & y_1^{\max} &= \min(Y, -\log \tau - y_2), & \tau &= M_{jj}^2/s
\end{aligned}$$

Fig. 2 shows jet-jet invariant mass distribution for the process  $pp \rightarrow D_2 \rightarrow jjX$  together with the estimation of the QCD background at the LHC. For comparison, signal peaks for vector diquark masses  $M_D = 2, 4, 6, 8$  TeV and  $\alpha_D = 0.1$  are superimposed on the background distribution.

We have estimated signal and background events for an integrated LHC luminosity of  $10^5 \text{ pb}^{-1}$  taking into account, as an example, the energy resolution of ATLAS hadronic calorimeter [12]:

$$\frac{\delta E}{E} = \frac{50\%}{\sqrt{E}} + 3\% \tag{11}$$

for jets with  $|y| < 3$ . The mass resolution can be expressed as [9]

$$\frac{\Delta M_{jj}}{M_{jj}} \approx \frac{\delta E}{\sqrt{2}E} \tag{12}$$

We have chosen  $2\Delta M_{jj}$  as the mass window centered at  $M_{jj}$  for signal and background estimations.

Number of signal (S), background (B) events and the corresponding significances for  $\alpha_D = 0.1$  are tabulated in Table III. Evidently, tighter cut on the rapidity  $y$  improves the significance considerably. In Table IV, we present the achievable mass limits for different values of  $\alpha_D$ . As discovery criteria, we adopt  $S/\sqrt{B} \geq 5$  and  $S \geq 25$ .

## V. CONCLUSIONS

The example of  $D_2$  shows that the resonance production of vector diquarks at the LHC has large cross section. With reasonable cuts, it may be possible to cover the region up to 9 TeV. The LHC potential for the discovery of  $D_2$  is clearly demonstrated in Fig. 3 where minimum integrated luminosities, needed to satisfy the adopted criteria, are plotted as a function of  $M_D$  for various  $\alpha_D$  values.

- 
- [1] H. Terazawa, Phys. Rev. 22 (1980) 184; H. Harari, Phys. Rep. 104 (1984) 159; D'Souza and Kalman, Preons, World Scientific Publishing, (1992).
  - [2] S. Sultansoy, hep-ph/0003269 (2000).
  - [3] J. Wudka, Phys. Lett. B167 (1986) 337.
  - [4] J.L. Hewett and T.G. Rizzo, Phys. Rep. 183 (1989) 193.
  - [5] F. Abe *et al.*, CDF Collaboration, Phys. Rev. Lett. 77 (1996) 5336; B. Abbott *et al.*, D0 Collaboration, Phys. Rev. Lett. 80 (1998) 666.
  - [6] D. Schaile and P.M. Zerwas: Proceedings of the Workshop on Physics at Future Accelerators, CERN Yellow Report 87-07, Vol. II, p.251 (1987).
  - [7] T.G. Rizzo, Z. Phys. C43 (1989) 223.
  - [8] V.D. Angelopoulos *et al.*, Nucl. Phys. B292, 59 (1987).
  - [9] S. Atağ, O. Çakır, and S. Sultansoy, Phys. Rev. D59, 015008 (1998).
  - [10] CTEQ Collaboration, H.L. Lai *et al.*, Eur. Phys. J. **C12** (2000) 375.
  - [11] Torbjörn Sjöstrand *et al.*, hep-ph/0010017 (2000).
  - [12] ATLAS Collaboration, ATLAS TDR 14, CERN/LHCC 99-14 (1999).

TABLE I. Quantum numbers of the first generation, color  $\bar{3}$  diquarks described by the effective lagrangian given in the text according to  $SU(3)_C \times SU(2)_W \times U(1)_Y$  invariance.  $Q_{em} = I_3 + Y/2$

Scalar Diquarks	$SU(3)_C$	$SU(2)_W$	$U(1)_Y$	$Q$	Couplings
$D_1$	$3^*$	1	2/3	1/3	$u_L d_L(g_{1L}), u_R d_R(g_{1R})$
$\tilde{D}_1$	$3^*$	1	-4/3	4/3	$d_R d_R(\tilde{g}_{1R})$
$\tilde{D}'_1$	$3^*$	1	8/3	-2/3	$u_R u_R(\tilde{g}'_{1R})$
$D_3$	$3^*$	3	2/3	$\begin{pmatrix} 4/3 \\ 1/3 \\ -2/3 \end{pmatrix}$	$\begin{pmatrix} u_L u_L(\sqrt{2}g_{3L}) \\ u_L d_L(-g_{3L}) \\ d_L d_L(-\sqrt{2}g_{3L}) \end{pmatrix}$
Vector Diquarks					
$D_{2\mu}$	$3^*$	2	-1/3	$\begin{pmatrix} 4/3 \\ 1/3 \end{pmatrix}$	$\begin{pmatrix} d_R d_L(g_2) \\ d_R u_L(-g_2) \end{pmatrix}$
$\tilde{D}_{2\mu}$	$3^*$	2	5/3	$\begin{pmatrix} 4/3 \\ 1/3 \end{pmatrix}$	$\begin{pmatrix} u_R d_L(\tilde{g}_2) \\ u_R u_L(-\tilde{g}_2) \end{pmatrix}$

TABLE II. Cross sections (pb) for QCD backgrounds contributing to j-j final states at parton level generated by PYTHIA 6.1 with various cuts.

Process	$p_T > 100$ GeV	$p_T > 500$ GeV	$p_T > 1000$ GeV	$p_T > 1500$ GeV	$p_T > 2000$ GeV
$gg \rightarrow gg$	$6.3 \times 10^5$	$2.0 \times 10^2$	$2.3 \times 10^0$	$8.6 \times 10^{-2}$	$5.7 \times 10^{-3}$
$q_i g \rightarrow q_i g$	$6.4 \times 10^5$	$4.8 \times 10^2$	$1.0 \times 10^1$	$6.4 \times 10^{-1}$	$5.7 \times 10^{-2}$
$q_i q_j \rightarrow q_i q_j$	$1.0 \times 10^5$	$1.8 \times 10^2$	$6.7 \times 10^0$	$6.3 \times 10^{-1}$	$8.8 \times 10^{-2}$
$gg \rightarrow q_k \bar{q}_k$	$2.4 \times 10^4$	$9.8 \times 10^0$	$1.0 \times 10^{-1}$	$4.9 \times 10^{-3}$	$2.9 \times 10^{-4}$
$q_i \bar{q}_i \rightarrow q_k \bar{q}_k$	$1.6 \times 10^3$	$2.8 \times 10^0$	$1.3 \times 10^{-1}$	$9.0 \times 10^{-3}$	$1.1 \times 10^{-3}$
$q_i \bar{q}_i \rightarrow gg$	$1.5 \times 10^3$	$2.5 \times 10^0$	$6.7 \times 10^{-2}$	$8.1 \times 10^{-3}$	$8.5 \times 10^{-4}$
Total	$1.4 \times 10^6$	$8.8 \times 10^2$	$1.9 \times 10^1$	$1.4 \times 10^0$	$1.5 \times 10^{-1}$

TABLE III. Observability of the vector diquark  $D_2$  with  $\alpha_D = 0.1$  at LHC for  $L_{int} = 10^5 \text{pb}^{-1}$ .

$M_D$ (TeV)	1	2	3	4	5	6	7	8	9
$ y  < 2$									
S	$7.7 \times 10^7$	$6.6 \times 10^6$	$1.1 \times 10^6$	$2.4 \times 10^5$	$5.0 \times 10^4$	$9.9 \times 10^3$	$1.7 \times 10^3$	$2.5 \times 10^2$	$2.7 \times 10^1$
B	$2.8 \times 10^8$	$5.6 \times 10^6$	$4.2 \times 10^5$	$5.4 \times 10^4$	$8.4 \times 10^3$	$1.4 \times 10^3$	$2.2 \times 10^2$	$3.0 \times 10^1$	$3.1 \times 10^0$
$S/\sqrt{B}$	4585	2787	1768	1027	545	266	118	46	16
$ y  < 1$									
S	$2.6 \times 10^7$	$2.8 \times 10^6$	$5.8 \times 10^5$	$1.3 \times 10^5$	$2.9 \times 10^4$	$6.1 \times 10^3$	$1.1 \times 10^3$	$1.6 \times 10^2$	$1.8 \times 10^1$
B	$2.5 \times 10^7$	$5.2 \times 10^5$	$4.0 \times 10^4$	$5.0 \times 10^3$	$7.9 \times 10^2$	$1.3 \times 10^2$	$2.1 \times 10^1$	$2.8 \times 10^0$	$3.0 \times 10^{-1}$
$S/\sqrt{B}$	5213	3946	2889	1842	1044	534	245	99	34

TABLE IV. Achievable diquark mass limits for different diquark-quark-quark couplings in the framework of discovery criteria given in the text. The rapidity cut  $|y| < 2$  is applied.

$\alpha_D$	$M_D$ (TeV)	S	B	$S/\sqrt{B}$
0.1	9	27	3.1	16.0
0.01	8	25	30	4.6
0.001	5	500	8400	5.4
0.0005	4	1200	540006	5.1

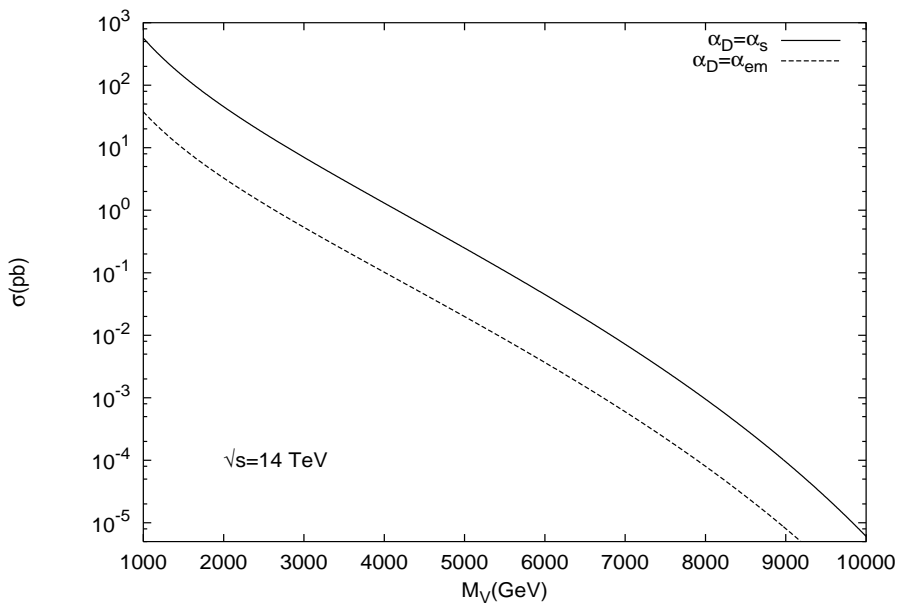


FIG. 1. Integrated cross section versus diquark mass for coupling strength  $\alpha_D = \alpha_s$  and  $\alpha_D = \alpha_{em}$ .

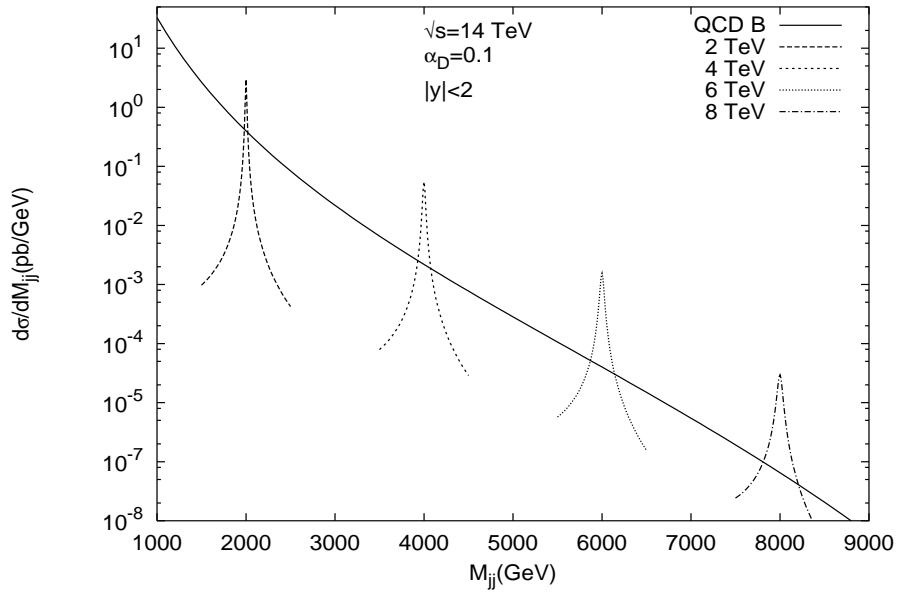


FIG. 2. Dijet invariant mass distribution for  $M_D = 2, 4, 6, 8$  TeV superimposed over the QCD background.

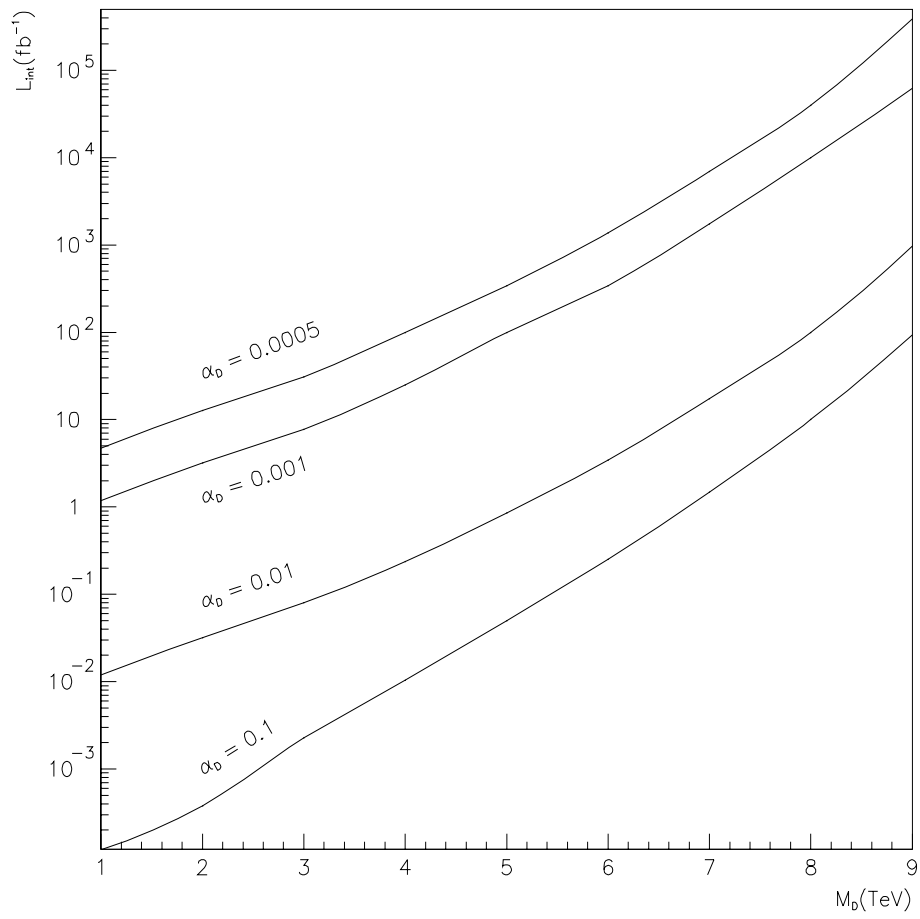


FIG. 3. The minimum integrated luminosities, needed to satisfy the adopted discovery criteria, as a function of  $M_D$  for various  $\alpha_D$  values.